IMPACT OF DIFFERENT TPMS TESSELATION APPROACHES ON MECHANICAL PROPERTIES OF PARTS

PATRIK DOBROVSZKY[1], TOMAS MACHAC[1], MAROS DUBNICKA[1], MATEJ PASAK[1], JOZEF BILIK[1], PETER POKORNY[1]

[1]Slovak University of Technology in Bratislava, faculty of Materials Science and Technology in Trnava

DOI: 10.17973/MMSJ.2024_06_2024015

Patrik.dobrovszky@stuba.sk

In the paper influence of several factors on shape accuracy and compressive strength of parts is analysed. First simulation software is used for prediction. Parts are cylindrical with 20 mm diameter, manufactured via SLA additive manufacturing technology. 1mm thick Gyroid TPMS structure is generated in cylinders with different volume % (30,40,50 %). Thanks to drainage holes it was possible to create parts that are hollowed, but have solid shell around and TPMS inside. Different tesselation approaches are tried (cylindrical and rectangural). Different radius of roundness is also tried on the surfaces joining tpms and shell of cylinder (0, 0.5, 1mm) Compression tests are then conducted and results are analysed in the form of graphs and colour map of deviations. Results are also compared with solid and fully hollow cylinders. Study finds that the maximum strength of the bodies is influenced by tessellation method, infill percentage, and blend radius. Higher infill percentages generally result in increased strength due to greater material volume transmitting loading force. While tessellation affects samples without shells, its impact is negligible on samples with shells.

KEYWORDS

TPMS, Stereolithography, Additive manufacturing, Gyroid, SLA, cylindrical, rectangular

1 INTRODUCTION

Triply periodic minimal surfaces (TPMS) are structures that have recently attracted much attention due to their biomimetic properties, which can be used in the automotive, aerospace or biomedical industries (Guo, X 2019; Liu, R 2023).

Triply Periodic Minimal Surfaces (TPMS) are mathematical surfaces that are periodic in three directions simultaneously. These surfaces have the unique property of being minimal, meaning they have the smallest surface area for a given enclosed volume. (Chen, L 2010)

These surfaces are characterized by geometrical and mechanical properties that are particularly important for their applications in fields such as tissue engineering (Guo, X 2019); (Li, Z 2023).

TPMS structures are categorized based on their topological properties, symmetries, and geometric characteristics. Recent research by Yan (Yan, Y 2017) has further expanded the understanding of TPMS families, highlighting the Gyroid, Schwarz P surfaces, Diamond, Primitive, and Sponge families among others. Each family exhibits unique geometric properties and symmetries, contributing to their diverse applications in different fields. For instance, the Gyroid structure, characterized by interconnected labyrinthine channels, has garnered interest in fields such as photonics and metamaterials due to its unique optical properties (Gibson, L 2001).

The mechanical properties of TPMS structures can be affected by many factors, including the solid angle and surface curvature (Li, Z 2023).

In a study by Dixit et al. in 2022, the author created a heat exchanger that was formed by a gyroid structure. For the fabrication of this heat exchanger, SLA additive manufacturing technology was used. The core of the TPMS structure with dimensions of 32.2 mm x 32.2 mm x 32.2 mm showed a decrease but also a temperature gain, where a heat exchange coefficient of 12-160 W/m2K was measured.

The paper by Sokolla (Sokollu, B 2022) investigates the mechanical behavior of gyroid, primitive and diamond TPMS lattice structures. The method that was used to fabricate these structures was the EBM method. The given samples exhibited a certain amount of dimensional error, with the gyroid structure exhibiting the highest and the diamond structure exhibiting the lowest dimensional error. Tensile tests were carried out, which showed that the diamond exhibited the highest UTS. In addition, the diamond showed the highest strength and the primitive the lowest strength. After FEM analysis was performed, results were obtained that were consistent with the tests performed.

Li in his paper evaluated the effect of solid angle and surface curvature. According to that paper, surface curvature is an important aspect that affects the mechanical properties. (Li, Z 2023b).

The mechanical properties of TPMS structures were also compared in the paper by Guo et al. where they were investigated on skeletal TPMS structures that were formed from cylindrical beams. Specifically, Young's modulus and ultimate strength were investigated. According to FEM simulations and experimental unidirectional compression tests, the Young's modulus and ultimate strength of both skeletal TPMS and TPMS structures are calculated as functions of relative density, thus they have a similar scaling law. (Guo, X 2019)

Mathematical algorithms offer precise means for crafting structures based on Triply Periodic Minimal Surfaces (TPMS), adhering to the definition of minimal surfaces. While various methods exist for designing TPMS, employing a level-set equation derived from a sum expressed in Fourier series stands out as the simplest and most commonly utilized approach for generating structures resembling minimal surfaces. These equations constitute a set of three-dimensional trigonometric functions that fulfill the equality condition $\phi(x,y,z) = 0$. (Yeranee, K 2022). The level-set equation of Gyroid structure that is used in this paper is described in Equation 1.

$$\phi(x,y,z)=\sin(x)\cos(y)+\sin(y)\cos(z)+\sin(z)\cos(x)=0 \quad (1)$$

This equation represents the intricate geometry of the Gyroid surface, capturing its characteristic interconnected channels and minimal surface properties.

In the study by Abouelmajd, (Abouelmajd, M 2022). the mechanical behavior of TPMSs based on rigid mesh lattice structures was investigated. Three unit cell geometries were considered, namely Neovius, Primitive and IWP. Unit cells were tested in two sizes, 1mm and 5mm, to evaluate the effect of unit cell size on mechanical performance. No effect of unit cell dimensions on mechanical response was found. It is evident that the mechanical properties of TPMS lattice structures depend on the selected relative density. The results obtained showed that the tensile strength of the IWP unit cell was higher than that of the Neovius and Primitive structures (Abouelmajd, M 2022).

The fabrication of TPMS structures in this paper was carried out using Stereolithography (SLA) additive manufacturing technology. SLA technology uses a laser beam that is gradually curing the respective resin layer in the Z-axis. Subsequently, once the layer is created, the platform is moved to create the next layer and the process continues until the entire 3D model is created. (Pagac, M 2021).

While previous studies have investigated the mechanical behavior and fabrication methods of TPMS structures (Dixit, T 2022; (Sokollu, B 2022), gaps still exist in understanding the influence of various factors on shape accuracy and compressive strength, particularly in the context of manufacturing processes such as SLA additive manufacturing technology. Therefore, the primary aim of this study is to analyze the influence of several factors on the shape accuracy and compressive strength of TPMS parts manufactured via SLA additive manufacturing technology.

Specifically, this study employs simulation software for predictive analysis, focusing on cylindrical parts with a 20 mm diameter. By generating 1 mm thick Gyroid TPMS structures within these cylinders at different volume percentages, the study explores the effects of tessellation approaches, and the radius of roundness on the surfaces joining the TPMS and shell of the cylinder. Through CT scanning and compression tests, the research aims to assess shape accuracy and compressive strength, comparing results with solid and fully hollow cylinders.

By addressing these aims, this study contributes to the understanding of TPMS structures and provides valuable insights into optimizing shape accuracy and mechanical performance in parts containing TPMS structures, thereby advancing their potential applications in various industries.

2 MATERIALS AND METHODS

2.1 Design and manufacture of samples

Gyroid TPMS structures were designed using combination of several CADs. Cylindrical samples with a diameter of 20 mm were used as the base for fabricating the TPMS structures. First the cylinders of 20 mm diameter were modeled in Fusion 360, then the cylinder was shelled so its shell thickness was 1 mm. Cylindrical infill body was then designed. This infill body was representing future TPMS structure. As a next step five holes with diameter of 2 mm were created on top and bottom surfaces of shell cylinder. These holes will be used as drainage holes, so the SLA resin will not be trapped inside the sample and they will also allow cleaning agent to enter the sample body and clean out any remaining non cured resin and clean the TPMS structure. Both the shelled cylinder and infill cylinder were then imported into nTop software together, they can be seen on Figure 1.

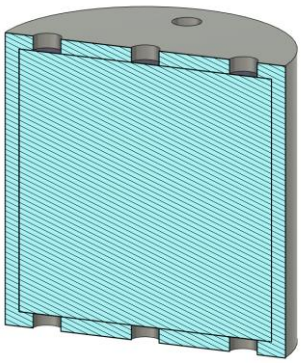

Figure 1. Shelled and infill cylinder

In the nTop software infill cylinder was converted into implicit body and Gyroid TPMS structure was generated via this body. There are several tessellation approaches possible for generating different TPMS structures. Some of those are along rectangural, cylindrical and spherical coordinate systems.

Rectangular volume lattice tessellation approach generates a lattice that fills a Volume by tessellating a unit cell along rectangural coordinates. Generally with this approach all that is needed to specify is unit cell size in all three axes and lattice thickness. Model of cylindrical sample with rectangular volume lattice is visible on Figure 2 (left).

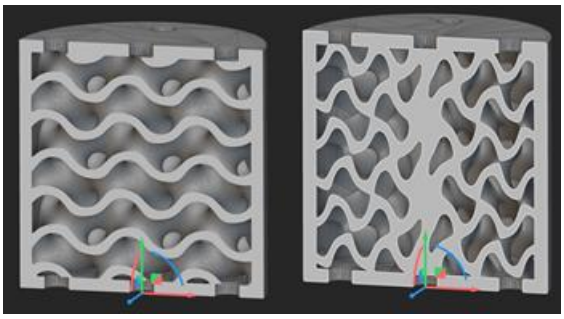

Figure 2. Samples with rectangular volume lattice (left) and cylindrical volume lattice (right)

Cylindrical volume lattice tessellation approach generates a lattice that fills a volume by tessellating a unit cell along cylindrical coordinates. With this approach parameters needed to specifiy the unit cell are cell radius and cell height. The cylindrical approach also generates so called arches, that sprout from the middle of the cylindrical unti outwards. Model of cylindrical sample with cylindrical volume lattice is visible on Figure 2 (right). For purposes of this paper walled TPMS structures were chosen instead of solid TPMS structures. Parameters for generating TPMS unit cells were chosen, so the resulting TPMS when combined with the shell body equals to 40, 50 and 60 vol. % of the whole sample. Blend radius between the TPMS and shell cylinder also plays important role in the mechanical properties of parts, since the mechanical stresses concentrate in the edges and corners, therefore the strength of the parts is predicted to increase with increasing blend radius, different values of blend radii compared on a cylindrical gyroid sample can be seen in Figure 3. The parameters for the samples can be seen in Table 1.

Tesselation approach	Blend radius (mm)	Desired vol. %	Actual vol. %
Rectangular volume lattice	0	60	60,06
Rectangular volume lattice	0,5	60	60,06
Rectangular volume lattice	1	60	60,06
Rectangular volume lattice	0	50	49,8
Rectangular volume lattice	0,5	50	49,8
Rectangular volume lattice	1	50	49,8
Rectangular volume lattice	0	40	39,98
Rectangular volume lattice	0,5	40	39,98
Rectangular volume lattice	1	40	39,98
Cylindrical volume lattice	0	60	59,4
Cylindrical volume lattice	0,5	60	59,4
Cylindrical volume lattice	1	60	59,4
Cylindrical volume lattice	0	50	49,7
Cylindrical volume lattice	0,5	50	49,7
Cylindrical volume lattice	1	50	49,7
Cylindrical volume lattice	0	40	40,7
Cylindrical volume lattice	0,5	40	40,7
Cylindrical volume lattice	1	40	40,7
Rectangular volume lattice no shell	x	60	60
Rectangular volume lattice no shell	x	50	50
Rectangular volume lattice no shell	x	40	40
Cylindrical volume lattice no shell	x	60	60
Cylindrical volume lattice no shell	x	50	50
Cylindrical volume lattice no shell	x	40	40
Shell only sample	x	x	x
Solid sample	x	x	x

Table 1. Design parameters of samples

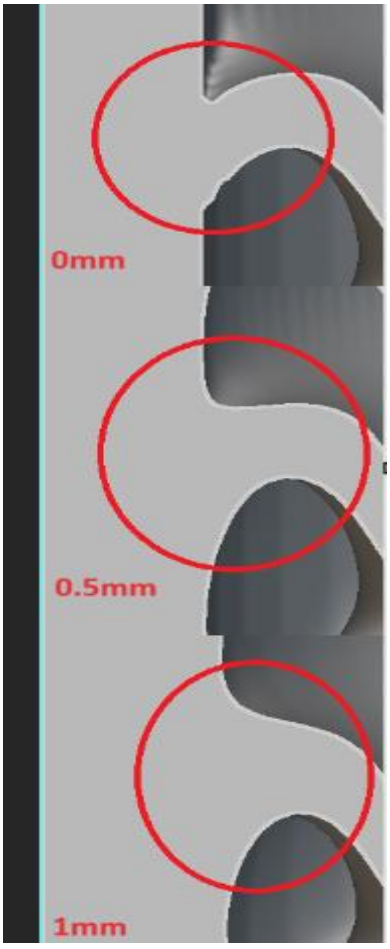

Figure 3. Different blend radius values

For comparative purposes samples containing no TPMS structures were also produced. These were produced in two versions, one made as solid sample other as shell only sample. There were also additionally created samples, that were containing only TPMS structures without shell, example of such can be seen on Figure 4.

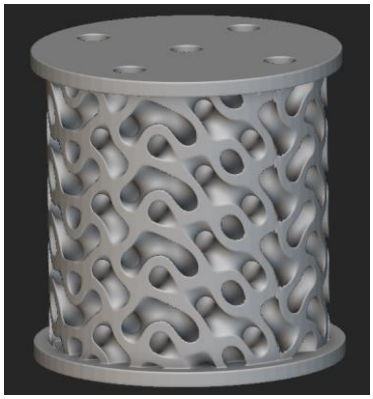

Figure 4. Sample without shell

The fabrication of TPMS structures was carried out using Stereolithography (SLA) additive manufacturing technology. A commercially available SLA 3D printer Formlabs form 3 was utilized for this purpose. Layer height used for manufacturing of the samples was 0,025 mm as it was necessary to achieve as precise TPMS structure as possible.

A Grey Pro V4 resin from Formlabs suitable for SLA printing was selected for fabricating the samples with TPMS structures. The resin and SLA technology offers high resolution and mechanical properties suitable for intricate geometries. SLA technology is layered laser based photopolymerization technology that solidifies resin in vat. Scheme of this technology can be seen on Figure 5.

2.2 *Simulational analysis*

In this study the FEM analysis was performed in software Autodesk Inventor Profesional 2024. Models of samples were inserted between two plates, while the top plate compresses the sample and bottom plate is rigid. The main goal of the analysis was to observe influence of applied loading force on used lattice structures and investigate differences in deformation behavior. The static stress analysis was used to simulate compression test. Due to complexity of internal structure used mesh settings were:

- Average elemental size – 0.100
- Minimum Element size – 0.200
- Grading Factor – 1.500
- Maximum Turn Angle – 60 degrees

The compression test with applied mesh is shown on fig.6

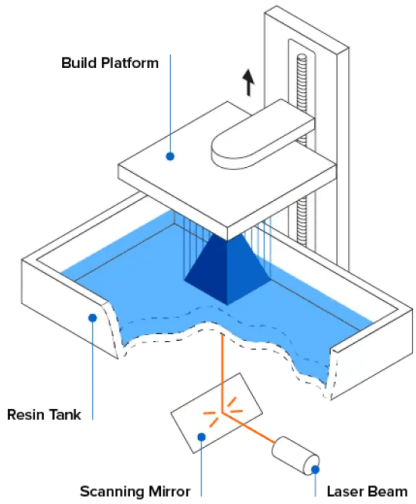

Figure 5. Scheme of SLA technology

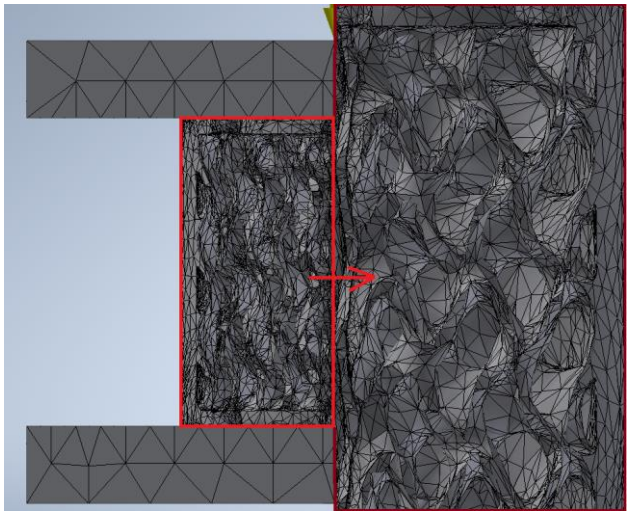

Figure 6. Section view of model with applied mesh

Static stress analysis setting was:

- Applied load force – 5000 N
- Contacts: Sliding / No separation – without friction
- Tolerance: 0,100 mm

The loading force was applied in the vertical axis of the sample on the top plate which compressed the sample and on the bottom plate the fixed constrains was applied which took all degrees of freedom that means this plate is rigid.

The material of print was FormLabs Grey Pro V4. This material is not available in Inventor material library, however its material properties are available from manufacturer. For the purpose of simulation, material Tough 2000 was edited and the material properties of FormLabs Grey Pro V4 were used in this material model which was subsequently used in analysis.

3 RESULTS

3.1 *Simulational analysis*

The material of print was FormLabs Grey Pro V4. This material is not available in Inventor material library. For the purpose of simulation, material Tough 2000 was edited and the material properties of FormLabs Grey Pro V4 was used in this material and was subsequently used in analysis. The Young's modulus of FormLabs Grey Pro V4 post-cured is 2.6 GPa and Ultimate Tensile Strength is 61 MPa, Poisson's ratio is 0.35.

From the results of simulations is obvious that distribution of Von Mises stress is very similar in both types of samples. Samples shows also the same deformation distribution. On Figure 7 and Figure 8 is shown distribution of Von Mises stress.

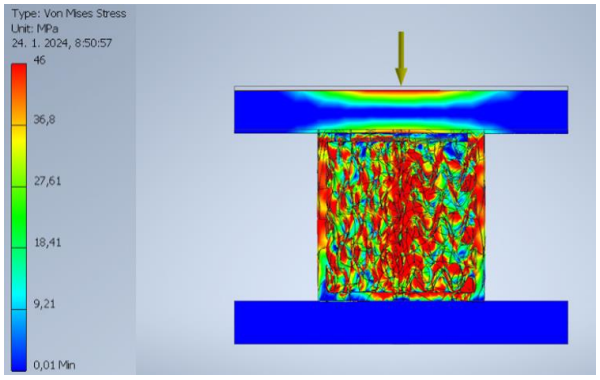

Figure 7. Von Misses stress distribution of sample Rectangle 50_0.5

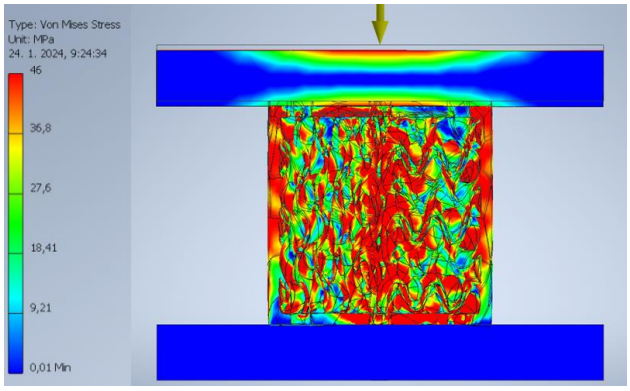

Figure 8. Von Misses stress distribution of sample Cylinder 50_0.5

On the other hand, samples with open lattice structures have different distribution of deformation and stress. This is caused by the fact that the structure is not connected to any walls as in Fig. 7 and 8 which lead to deformation in whole structure during deformation. Distribution of Von Misses stress of open lattice structure is on Fig 9.

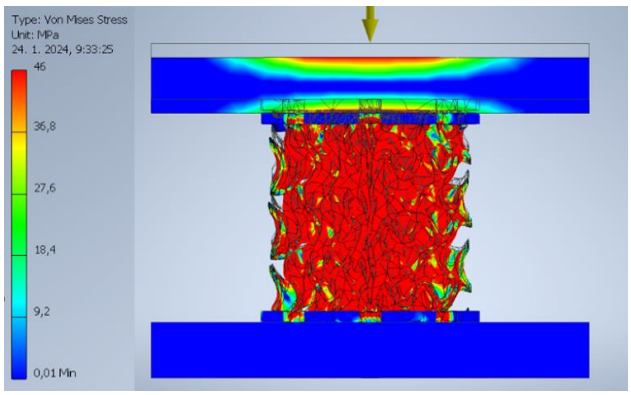

Figure 9. Von Misses stress distribution of sample Rectangle 50_X

This means that closing the lattice structure into the shell should improve overall resistance to deformation and strength. This fact we can also observe in maximum displacement. The values of maximum displacement is shown in Table.2.

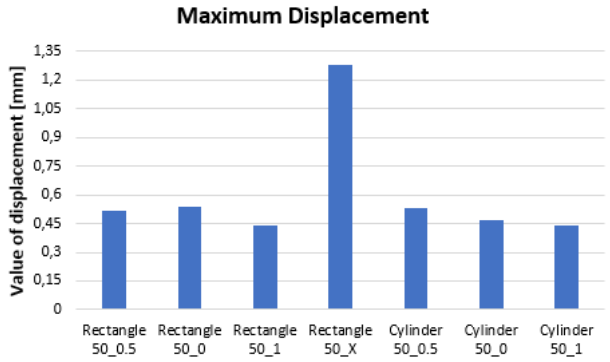

Table 2. **Maximum displacement in samples**

The only missing sample is Cylinder 50.X because this sample was not possible simulate because of open lattice structure which have very small areas and solver was not able to calculate deformations.

3.2 Experimental analysis of mechanical properties

The press test was performed on a universal machine LaborTech LabTest5.250SP1-VM. The displacement speed of the pushed contact discs was 10 mm.min-1 . The force increased slowly and gradually until it reached its maximum when the material broke. Each group of sample was measured three times, from which were calculated the mean value and standard error of the mean. Figure 10 and 11 shows the measured values of the maximum forces.

Figure 10 shows a comparison of maximal force between shell and solid body. Shell body with a wall thickness of 1 mm is close to 0% infill with thin wall. The solid body is filled with 100% material, which, in the calculation of the force acting on the homogeneous area of a cylinder with a diameter of 20 mm, gives a value of the press strength of the material as 204 ± 19 MPa.

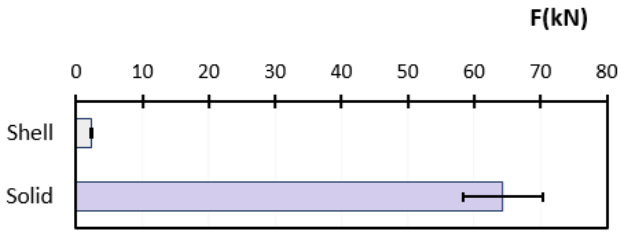

Figure 10. Comparison of maximal force of shell body and a solid body

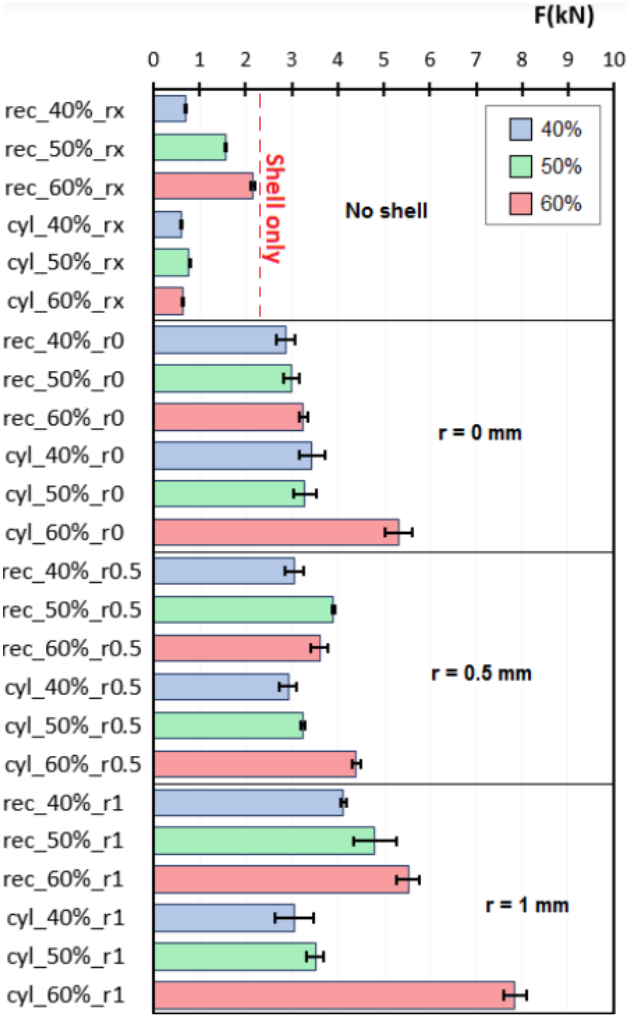

Figure 11. Comparison of the strength of different tessellation body

Figure 11 shows the maximum of compression force of the various tessellations. The bodies were divided into several groups according to the method of formation of the gyroid. Gyroid was created using by rectalgular (denoted “rec”) or cylinder (denoted “cyl”). Furthermore, the structures were created with different amount of infill 40%, 50%, 60%. The last variation is different radius of filet of the tpms joining and shell of cylinder as r = 0 mm; r = 0.5 mm and r = 1 mm (denoted “r”). All the bodies mentioned so far are covered with shell. Bodies without a shell are denoted with an “x” symbol. Figure 12 shows the same results, but separated into vol. % categories with increasing blend radius.

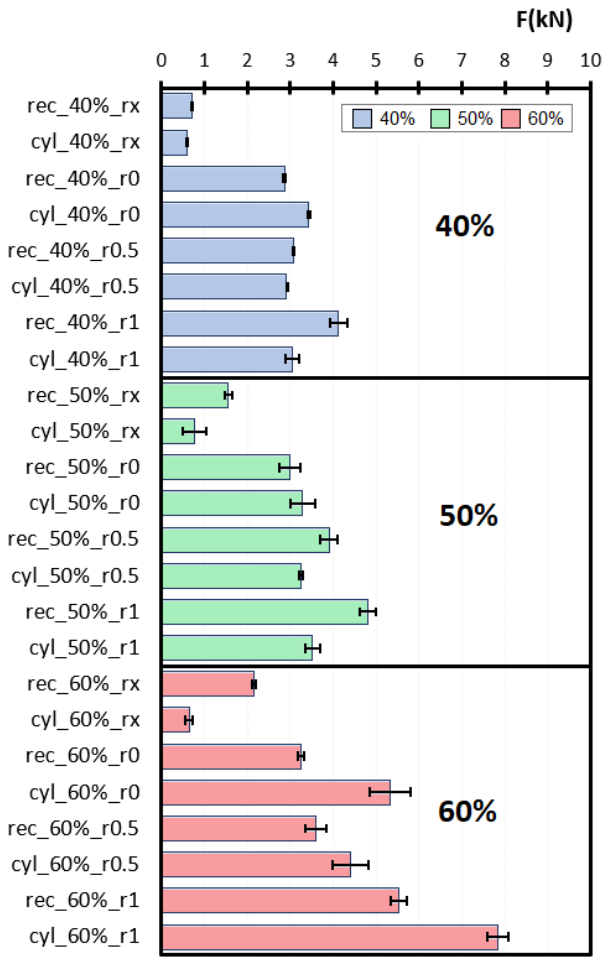

Figure 12. Comparison of the strength with increasing blend radius

Since the different gyroid shapes do not have a continuous cross-sectional area, only the maximum forces during the pressure test are compared. As expected, the highest loading capacity for all groups of different teselation were always achieved by bodies with 60% filling, because they contain the most material, which transmits the greatest amount of loading force. The smallest value is achieved by the groups with the lowest filling of 40% because they contain the least material. Filling 50% sometimes gives an increase and sometimes a decrease in maximum power. To generate a gyroid with different shape and degree of infill, which ultimately affects the size and shape of the tpms joints, which in turn affect the crosssection area.

It is apparent from the results, that the tessellation method does not have any significant effect on the mechanical properties when using TPMS as infill for solid parts. When we look at the parts without shell, there it is possible to see, that the rectangular TPMS achieves better results. As was expected, with the increasing blend radius also comes increase in loading capacity. However it is not known whether the increase is because the blend radius is better at distributing forces, or because with the radius a little bit of extra material is added to the structure.

4 CONCLUSIONS

The findings demonstrate that closing lattice structures into a shell enhances the strength and resistance to deformation of printed materials. Samples with closed lattice structures or solid bodies exhibit lower displacement and similar Von Mises stress distribution compared to those with open lattice structures. This suggests that the shell configuration provides structural support, leading to improved resistance to deformation and overall strength. Therefore, the design strategy of enclosing lattice structures within a shell is effective in enhancing the mechanical properties of printed materials.

The maximum strength of the bodies varies based on the method of tessellation, infill percentage, and blend radius. Bodies with higher infill percentages generally exhibit higher strength due to containing more material to transmit loading force.

The effect of tessellation is visible on the samples where no shell was used, but there was no effect visible on the samples with shell. With the higher vol.% of infill there is trend where the cylindrical approach offers higher strength, but it is possible that it is due to the arc count being increased when designing the part.

Effect of blend radius on strength is visible as expected. With increasing blend radius it is possible to see increased strength in samples. But it is not known whether it is because the blend radius offer better force distribution throughout the sample or whether it is because of the slight material increase inside the part.

ACKNOWLEDGMENTS

VEGA 001STU-4/2022

Support of the distance form of education in the form of online access for selected subjects of computer aided study programs.

REFERENCES

[Abouelmajd, M 2022] Abouelmajd, M., El Khadiri, I., Ezzaraa, I., Zemzami, M., El Afi, M., Lagache, M., Almangour, B., Arroub, I., Bouferra, R., Essaleh, M., Bahlaoui, A., Hmina, N., & Belhouideg, S. (2022). Mechanical Behavior of TPMS-Based Solid Network Structures Obtained by Additive Manufacturing Technology. 8th International Conference on Optimization and Applications, ICOA 2022 - Proceedings. https://doi.org/10.1109/ICOA55659.2022.9934585

[Chen, L 2010] Chen, L., Liu, J., & Hu, J. (2010). Applications of triply periodic minimal surfaces in material science. Materials Science and Engineering: A, 527(29-30), 7821-7826.

[Dixit, T 2022] Dixit, T., Al-Hajri, E., Paul, M. C., Nithiarasu, P., & Kumar, S. (2022). High performance, microarchitected, compact heat exchanger enabled by 3D printing. Applied Thermal Engineering, 210. https://doi.org/10.1016/j.applthermaleng.2022.118339

[Guo, X 2019] Guo, X., Zheng, X., Yang, Y., Yang, X., & Yi, Y. (2019b). Mechanical behavior of TPMS-based scaffolds: a comparison between minimal surfaces and their lattice structures. SN Applied Sciences, 1(10). https://doi.org/10.1007/s42452-019-1167-z

[Li, Z 2023] Li, Z., Chen, Z., Chen, X., & Zhao, R. (2023a). Mechanical properties of triply periodic minimal surface (TPMS) scaffolds: considering the influence of spatial angle and surface curvature. Biomechanics and Modeling in Mechanobiology, 22(2), 541–560. https://doi.org/10.1007/s10237-022-01661-7

[Liu, R 2023] Liu, R., Chen, W., & Zhao, J. (2023). A Review on Factors Affecting the Mechanical Properties of Additively-Manufactured Lattice Structures. In Journal of Materials Engineering and Performance. Springer. https://doi.org/10.1007/s11665-023-08423-1

[Pagac, M 2021] Pagac, M., Hajnys, J., Ma, Q.-P., Jancar, L., Jansa, J., Stefek, P., Mesicek, J. (2021). A Review of Vat Photopolymerization Technology: Materials, Applications, Challenges, and Future Trends of 3D Printing. Polymers 2021, 13(4), 598. doi:10.3390/polym13040598.

[Sokollu, B 2022] Sokollu, B., Gulcan, O., & Konukseven, E. I. (n.d.). Mechanical Properties Comparison of Strut-Based and Triply Periodic Minimal Surface Lattice Structures Produced by Electron Beam Melting. https://ssrn.com/abstract=4150322

[Yan, Y 2017] Yan, Y., Cai, H., & Yin, J. (2017). Recent progress in the study of triply periodic minimal surfaces and related structures. Crystals, 7(8), 244.

[Yeranee, K 2022] Yeranee, K.; Rao, Y. A Review of Recent Investigations on Flow and Heat Transfer Enhancement in Cooling Channels Embedded with Triply Periodic Minimal Surfaces (TPMS). Energies 2022, 15, 8994. https://doi.org/10.3390/ en15238994

CONTACTS:

Ing. Patrik Dobrovszký

Slovak University of Technology in Bratislava, faculty of Materials Science and Technology in Trnava

patrik.dobrovszky@stuba.sk

tomas.machac@stuba.sk

maros.dubnicka@stuba.sk

matej.pasak@stuba.sk

jozef.bilik@stuba.sk

peter.pokorny@stuba.sk